

SLAC {PUB {7915
 OUNP {99{06
 Saclay/SPhT -T 99/047
 PITTA 99/12
 May 1999

MEASUREMENT OF THE RUNNING b-QUARK MASS USING $e^+e^- \rightarrow b\bar{b}$ EVENTS

A. Brandenburg¹, P.N. Burrows², D.M. Muller³, N. Oishi⁴, P. Uwer⁵

ABSTRACT

We have studied the determination of the running b-quark mass, $m_b(M_Z)$, using Z^0 decays into 3 or more hadronic jets. We calculated the ratio of 3-jet fractions in $e^+e^- \rightarrow b\bar{b}$ vs. $e^+e^- \rightarrow q\bar{q}$ ($q = u$ or d or s) events at next-to-leading order in perturbative QCD using six different infrared-and collinear-safe jet-finding algorithms. We compared with corresponding measurements from the SLD Collaboration and found a significant algorithm-dependence of the fitted $m_b(M_Z)$ value. Our best estimate, taking correlations into account, is $m_b(M_Z) = 2.52 \pm 0.27 \text{ (stat.)}^{+0.33}_{-0.47} \text{ (syst.)}^{+0.54}_{-1.46} \text{ (theor.) GeV/c}^2$.

¹ Institut für Theoretische Physik, RWTH Aachen, D-52056 Aachen, Germany and DESY Theory Group, D-22603 Hamburg, Germany.

² Oxford University, Particle and Nuclear Physics, Oxford, OX1 3RH, UK.

³ Stanford Linear Accelerator Center, 2575 Sand Hill Road, Menlo Park, CA 94025, USA.

⁴ Nagoya University, Nagoya 464, Japan.

⁵ Service de Physique Théorique, Centre d'Etudes de Saclay, F-91191 Gif-sur-Yvette cedex, France.

1. Introduction

Three-jet events of the type $e^+ e^- \rightarrow q\bar{q}g$ provide an ideal laboratory for making precise tests of Quantum Chromodynamics (QCD) [1]. Since the initial state is free of strongly-interacting particles the experimental environment is intrinsically 'clean', and the process is more amenable to calculation using perturbation theory than, for example, multi-jet final states in hadron-hadron or lepton-hadron collisions. A number of perturbative QCD (pQCD) predictions for 3-jet dominated hadronic event-shape observables, for massless quarks, complete at next-to-leading order (NLO) are available [2, 3, 4, 5, 6, 7, 8].

One would expect the emission of gluon radiation in events containing massive quarks, $e^+ e^- \rightarrow Q\bar{Q}g$ ($Q = b$ or c), to be modified relative to that in $e^+ e^- \rightarrow q\bar{q}g$ ($q = u$ or d or s) events due to the restriction in phase space imposed by the non-zero quark mass. One would also expect such a modification to depend on the choice of the event-shape observable, and to be potentially relatively large for those observables in which the quark-jet mass enters kinematically into the definition. Recently NLO calculations of $e^+ e^- \rightarrow Q\bar{Q}g$ have been performed in which quark mass effects have been taken into account explicitly [9, 10, 11]. From these calculations one expects the size of the mass effects in $c\bar{c}g$ events at $\frac{p}{s} = M_c$ to be rather small, at the level of 1%. However, for $b\bar{b}g$ events the relative size of the b-mass effects on event-shape observables can be much larger, up to around 5%. Such a large effect needs to be taken into account in precise studies of $b\bar{b}g$ events where the experimental errors can be comparable with, or smaller than, this size.

For example, tests of the flavour-independence of strong interactions involve measurements of the ratios $r^Q(X) = X^Q/X^{\text{uds}}$ of a 3-jet observable X in $Q\bar{Q}g$ versus $q\bar{q}g$ events. Currently the experimental errors on $r^b(X)$ are of the order of 1-2%, and b-mass effects are clearly visible in the data [12, 13]. By contrast, the errors on $r^c(X)$ are much larger than 1% and any c-mass effects are not discernible. Hence, in recent

measurements the NLO massive calculations have been employed to correct $r^b(X)$ for the mass effects, so as to determine the ratio of strong couplings, $\frac{b}{s} = \frac{uds}{s}$ [14, 15], and test the ansatz of colour-independence of strong interactions.

An alternative, and a priori equally valid, approach is to assume that strong interactions are colour independent, and use the sensitivity of event-shape observables to mass effects to determine the mass itself. In the theoretical prediction one has the freedom to choose the renormalization scheme which defines the quark mass. For example, one can write the NLO result in terms of either the perturbative pole mass M_b or the 'running' mass $m_b(\mu)$. The latter is defined by the modified minimal subtraction (\overline{MS}) scheme [16] employed to renormalize the mass at a scale μ . At the Z^0 scale, M_z , the running mass is preferable because large logarithms of the form $\ln(M_b^2/M_z^2)$ are absorbed in $m_b(M_z)$, and the perturbative expansion is thus improved. The DELPHI collaboration has recently studied the 3-jet-rate $R_3(y_c)$, where R_3 was determined using the Durham (D) jet-finding algorithm [17], and y_c is the scaled-invariant-mass criterion which determines the jet multiplicity. From their measurement of $r^b(R_3)$ at $y_c = 0.02$ DELPHI obtained [13]:

$$m_b(M_z) = 2.67 \quad 0.25 \text{ (exp:)} \quad 0.34 \text{ (frag:)} \quad 0.27 \text{ (theor:)} \text{ GeV}^2/c \quad (1)$$

Such 3-jet-event observables have been used for many years to determine $\frac{b}{s}(M_z)$ from inclusive-electron-annihilation events [18]. Though the $\frac{b}{s}$ value obtained by fitting a NLO pQCD calculation to any one measured observable can have quite a small experimental error, 0.001 for some observables, there is a strong dependence of the fitted $\frac{b}{s}(M_z)$ value on the choice of observable [19, 20]. This spread of values leads to a large and dominant uncertainty on $\frac{b}{s}(M_z)$ determined with this technique [18]. Since non-perturbative effects are supposedly taken into account in these measurements, usually by applying corrections based on well-tested hadronisation models [21], a consistent description within the framework of pQCD is viable only if one postulates large (and uncalculated) next-to-next-to-leading-order (NNLO) contributions to the observables. Hence, in this picture, the spread in $\frac{b}{s}(M_z)$ values determined at NLO results from

the omission of the uncalculated higher-order terms. Furthermore, it can be argued that a strong dependence of a NLO calculation on the renormalisation scale is generally a sign of large NNLO contributions. Such a dependence is indeed observed for most of the observables [19, 20, 22], and supports the previous interpretation, though there is little consensus on a procedure for quantifying the scale-dependence of measurements of $s(M_Z)$.

The DELPHI determination of $m_b(M_Z)$ (Eq. 1) is based on a ratio of 3-jet-event observables calculated at NLO. Given this apparently very precise result derived from one observable, it is interesting to consider the possible effect of NNLO contributions. Naively one might expect any potentially sizeable effects in the numerator and denominator largely to cancel. However, a residual uncertainty at only the 2% level on r^b corresponds (Section 3) to a 0.5 GeV/c² error on $m_b(M_Z)$, which is comparable with the quoted total error on the DELPHI measurement. For the purpose of investigation we have studied the extraction of $m_b(M_Z)$ from the ratios $r^b(R_3)$, where R_3 was determined using six different infra-red- and collinear-safe jet-finding algorithms. As in the case of $s(M_Z)$ measurements using such observables, the study of an ensemble of results from different observables, all calculated at NLO, may uncover systematic effects relating to the uncalculated NNLO contributions. We used the Durham and Geneva (G) [23] schemes, and the E, E0, P and P0 variations of the JADE algorithm [24] to evaluate the mass-dependent NLO pQCD predictions¹, and compared them with the corresponding experimental measurements published by the SLD Collaboration [14].

In Section 2 we outline the theoretical framework and briefly describe the NLO calculations used here. In Section 3 we compare the calculations with the data and extract values of $m_b(M_Z)$ using each jet algorithm in turn. We compare the results obtained using the different jet algorithms, and discuss the systematic uncertainties. In Section

¹ Note that in events containing quarks of mass m , for $y_c = m^2/s$ the E, E0, P, P0 algorithms can not be used to define infra-red-safe massive 3-jet fractions. This is because the clustering metric for these algorithms is given by $y_{ij} = (p_i + p_j)^2/s$, which for a pair consisting of a gluon and a massive quark is m^2/s even for arbitrarily soft gluons.

4 we combine these results to obtain our best estimate of the central m_b (M_Z) value and error by taking correlations into account. These results supersede the preliminary results presented in [12].

2. Theoretical Framework

In this section we describe the computation of the double ratio:

$$r^b(y_c) = R_3^b(y_c) = R_3^{uds}(y_c); \quad (2)$$

where we define $R_3^q(y_c)$ to be the fraction of events classified as containing 3 or more jets with a particular jet-finding algorithm at a particular y_c value. The event flavour is defined by the flavour of the primary quarks that couple to the Z^0 . This definition means that events of the type $Z^0 + q\bar{q}g + q\bar{q}bb$ are classified as light-quark events².

$R_3^b(y_c)$ and $R_3^{uds}(y_c)$ can be written to NLO accuracy:

$$R_3^q(y_c) = \frac{s}{2} A^q(y_c) + \frac{s}{2}^2 (B^q(y_c) + C^q(y_c)) + O\left(\frac{3}{s}\right); \quad (3)$$

where the coefficients A (B) represent the LO (NLO) contribution to 3-jet production, and the coefficients C represent the LO contribution to 4-jet production. Thus we have (we suppress here the argument y_c):

$$r^b = \frac{A^b}{A^{uds}} + \frac{s}{2} \frac{B^b + C^b}{A^{uds}} - \frac{B^{uds} + C^{uds}}{A^{uds}} \frac{A^b}{A^{uds}}^! + O\left(\frac{2}{s}\right); \quad (4)$$

A. 3-jet Contributions

For 3-jet production the LO massless (A^{uds}) and massive (A^b) [25] as well as the NLO massless (B^{uds}) [3] coefficients are well known. In order to calculate the massive NLO

²This distinction is possible only because there are no contributions to R_3^q from the interference of the amplitudes for $Z^0 + q\bar{q}g + q\bar{q}bb$ and $Z^0 + b\bar{b}g + b\bar{b}q\bar{q}$.

coefficient B^b we need the matrix elements for

$$e^+ e^- \rightarrow (; z) \rightarrow b \bar{b} g \quad (5)$$

to order $\frac{1}{s^2}$, as well as the matrix elements for the parton processes

$$e^+ e^- \rightarrow (; z) \rightarrow b \bar{b} g g; b \bar{b} q \bar{q}; b \bar{b} b \bar{b} \quad (6)$$

In the calculation of the virtual corrections to Eq. 5 both ultra-violet (UV) and infra-red (IR) singularities are encountered. The UV singularities are removed by the usual renormalization procedure of the mass parameter and the QCD coupling α_s .

The IR singularities are cancelled by the real contributions from the processes listed in Eq. (6). It is worthwhile adding some remarks about this cancellation. Today it is more or less standard to regulate the IR divergences in the framework of dimensional regularization. To cancel the divergences in the virtual corrections one must then integrate the real contributions over some regions of phase-space in dimensions. More precisely one must integrate over the regions where a gluon is soft or two massless partons are collinear. In general this would be a formidable task. Therefore several techniques have been developed in the past (see for example [4, 5, 6, 26]) to simplify this problem using the general factorization properties of QCD amplitudes. In the calculation reported in [9] on which the current paper is based the so called phase-space-slicing method [4] was used. The same is true for the results presented in [10] on which the DELPHI analysis [13] is based. In the calculation given in [11] an alternative, the so-called subtraction method, was used.

In the simplest version of the phase-space slicing method one separates the 'soft' and 'collinear' regions (often called 'unresolved regions') from the rest of the phase-space ('resolved regions') by demanding a minimal invariant mass-squared s_{min} for all pairs of partons. In the soft and collinear regions the squared matrix elements can be approximated by the use of the soft and collinear factorization which is valid in the appropriate limits. After this simplification the relevant part of the squared matrix elements can be integrated analytically in dimensions. The phase-space integration

over the resolved regions can be done numerically in four dimensions. In the case of massive quarks the phase-space slicing method must be modified, although the basic features are the same. In particular, the 'slicing' between the soft/collinear regions and the regions where all partons are hard can still be parametrized in terms of one variable s_{min} .

The approximation used in the unresolved region is only valid for small values of s_{min} . On the other hand for small s_{min} large cancellations between the numerically integrated and the analytically integrated parts will arise leading to possible errors in the sum of the two. Note that the artificial cut parametrized by s_{min} is not related to any physical cut. Thus the theoretical prediction must be independent of s_{min} . In practice, for the NLO coefficient B^b this will be true up to corrections of the order of $s_{\text{min}}=s$. With the value $s_{\text{min}} = 0.5 \text{ GeV}^2$, which we have used in our calculation, the systematic error in B^b due to the phase-space slicing method is negligible compared with the numerical error due to the numerical integration, which is itself negligibly small.

For technical reasons it is easier to perform the calculation of r^b first in the pole mass scheme, and switch to the running mass afterwards. The relation between the pole mass M_b and the $\overline{\text{MS}}\text{ mass } m_b(\tau)$ reads

$$M_b = m_b(\tau) + \delta m_b(\tau); \quad (7)$$

where, to order s ,

$$m_b(\tau) = -\frac{s}{3} - \frac{4}{3} \ln \frac{m_b^2(\tau)}{2} \delta m_b(\tau); \quad (8)$$

This implies the following relation between r^b in both mass renormalization schemes [27]:

$$r^b(M_b) = r^b(m_b(\tau)) + \frac{1}{A^{\text{uds}}} m_b(\tau) \frac{dA^b(m_b(\tau))}{dm_b(\tau)} + O(\frac{2}{s}); \quad (9)$$

The mass dependence of A^b can be written as $A^b(m_b) = A^{\text{uds}} + A^b(m_b)m_b^2/s$, which defines the function $A^b(m_b)$. For $m_b^2 \ll s$, A^b depends only weakly on m_b . Ignoring

this residual mass dependence we have

$$\frac{1}{A_{uds}} m_b(\mu) \frac{dA^b(m_b(\mu))}{dm_b(\mu)} = \frac{1}{A_{uds}} A^b \frac{q}{m_b^2(\mu) + 2m_b(\mu) m_b(\mu)} = A^b(m_b(\mu)); \quad (10)$$

and we use the r.h.s. of (10) to convert the results for r^b from the pole mass to the \overline{MS} mass renormalization scheme. This excellent approximation avoids the calculation of the derivative dA^b/dm_b for each algorithm.

B . 4-jet C ontributions

Both the massless [3] and massive [28] LO 4-jet fraction contributions (C) are well known. Recently, the massless 4-jet fraction has been computed to NLO [29]. These corrections, which are of order $\frac{3}{s}$ and therefore not included in our prediction for r^b , can change, depending on the jet algorithm, the values of the massless C coefficients by up to 100%. Note that part of these large NNLO corrections to r^b will cancel between the massless and (yet unknown) massive $O(\frac{3}{s})$ C coefficients entering (4).

C . C alculation of r^b

The calculation of r^b was performed, for each of the six jet algorithms at the optimal values (discussed below), for $m_b(M_z)$ values in the range $2.0 \leq m_b(M_z) \leq 5.0$ GeV/c. These predictions are shown as points in Fig. 1. The renormalization scale was set to $\mu_s = s$ and we used $\mu_s(M_z) = 0.118$. The dependence of r^b on the renormalization scale is trivial if r^b is expressed in terms of the pole mass M_b ; it enters only through the running of μ_s . An additional dependence is introduced if one switches to the running mass $m_b(\mu)$ by using Eq. (9). The theoretical uncertainty on $m_b(M_z)$ due to the choice of the renormalization scale will be discussed in section 3.

The function

$$f(m) = 1 + \frac{m^2}{s} + \frac{m^2}{s} \ln \frac{m^2}{s} + \frac{m^4}{s^2} \quad (11)$$

where r^b and r^0 are free parameters, was fitted to these points. The ansatz (11) can be justified as follows: 1) As $m \rightarrow 0$, the massive fraction R_3^b approaches the massless one³ R_3^{uds} ; 2) since $m^2 \ll s$, it is a very good approximation to keep only the leading terms in m^2/s . The fitted parameter values are listed in Table 1; the functions are shown in Fig. 1 and provide a good description of the mass dependence of the calculations.

Algorithm			
E	207.6	16.10	13029.9
E0	42.2	3.58	3881.3
P	211.7	28.51	5060.9
P0	236.8	30.95	3417.6
D	79.3	17.16	4610.8
G	89.6	11.04	3229.9

Table 1: Fitted parameters of the function $f(m) = 1 + m^2/s + (m^2/s) \ln(m^2/s) + m^4/s^2$ for each jet algorithm.

It can be seen that the $m_b(M_z)$ -dependence varies according to the jet algorithm. For $m_b(M_z) = 2.0 \text{ GeV}/c$, $r^b > 1$ and the slope is positive for the E, E0, P and P0 cases, whereas $r^b < 1$ and the slope is negative for the D and G cases. This can be understood qualitatively in terms of two competing physical origins. First, the non-zero b-mass tends to cause a phase-space suppression of gluon emission relative to the massless quark case, implying $r^b < 1$. Second, for a given kinematic configuration, the large b-mass tends to enhance the invariant mass of a local quark-gluon pair relative to the massless quark case. Since the JADE family of jet algorithms is based on a clustering metric that is closely related to invariant mass, for fixed y_c the two partons are more likely to be resolved as separate jets when the quark is massive, implying

³This is true up to differences induced by triangle diagrams [30], which lead to deviations of the $r^b(m=0)$ from 1 of less than 0.1%.

r^b 1. By contrast, the clustering metric used in the Durham and Geneva algorithms is less sensitive to this kinematic effect, the phase-space suppression dominates, and

r^b 1. For increasing values of y one expects both effects to diminish in importance and $r^b \rightarrow 1$. For the D algorithm this has been observed in the DELPHI study [13].

3. Extraction of the b-Quark Mass

We used measurements of r^b published [14] by the SLD Collaboration. These measurements are based on a sample of 150,000 hadronic Z^0 decays recorded between 1993 and 1995, for which the original 120-million pixel CCD vertex detector was used for event flavour separation. SLD has subsequently recorded a further 400,000 Z^0 decays with a new 307-million-pixel vertex detector, and it would be straightforward to repeat the present analysis when the new data are made available. Though not as statistically powerful as the DELPHI result for the D jet algorithm, the SLD published data include results for the six different jet algorithms D, G, E, E0, P and P0, and are hence suitable for this study of possible observable-dependent systematic effects.

Full details of the experimental procedure are given in [14]. Briefly, $e^+e^- \rightarrow$ hadrons events were selected, and a flavour-tagging algorithm was applied to select samples of events of primary b, c, and uds quark flavour. The algorithm was based on the mass and momentum of secondary decay vertices reconstructed using the vertex detector. Light-quark (uds) events rarely contain reconstructed secondary decay vertices, and these typically result from strange particle decays and are of low mass. Conversely, bb events typically contain high-mass vertices from B-hadron decays. The purity of the b-tagged (uds-tagged) event sample was 90% (91%) respectively.

Each jet-finding algorithm was applied in turn to the uds- and b-tagged samples and, for each algorithm, the ratios (Eq. 2) were formed. The ratio is an attractive quantity as many of the experimental and theoretical systematic uncertainties effectively cancel.

Each ratio was then corrected for the effects of detector acceptance and resolution, the bias of the flavour tag to select preferentially 2-jet rather than 3-jet events, the flavour compositions, and hadronisation effects. For each algorithm an 'optimal' y_c value was selected so as to minimise the combined statistical and experimental systematic error.

The measured r^b values and the associated errors are listed in Table 2 [14]. The central values and statistical errors are also shown in Fig. 1. The set of r^b values is not consistent with unity, which indicates that the mass effects are significant. Furthermore, a systematic algorithmic dependence is apparent, with $r^b = 1$ for the JADE family of algorithms and $r^b < 1$ for the D and G algorithms, in agreement with the expectations discussed in Section 2.

Algorithm	y_c	r^b	stat.	exp. syst.	had.
E	0.040	1.050	0.026	+ 0.038 - 0.042	+ 0.011 - 0.046
E0	0.020	1.054	0.019	+ 0.030 - 0.037	+ 0.007 - 0.045
P	0.020	1.048	0.019	+ 0.027 - 0.037	+ 0.002 - 0.026
P0	0.015	1.055	0.017	+ 0.028 - 0.035	+ 0.007 - 0.037
D	0.010	0.964	0.023	+ 0.038 - 0.041	+ 0.001 - 0.006
G	0.080	0.995	0.032	+ 0.035 - 0.036	+ 0.020 - 0.008

Table 2: SLD measured values and errors of r^b .

For each jet algorithm, by comparing the theoretical curve in Fig. 1 with the SLD data, one can read off the preferred $m_b(M_Z)$ value. The central values are listed in Table 3. In each case upper and lower statistical errors were evaluated from the crossing points of the error band with the theoretical prediction, except in the case of the G algorithm, for which the upper statistical bound is consistent with $m_b = 0$; in this case an error equal to the central value was assigned. Each experimental systematic error on r^b [14] was similarly transformed into a systematic error on $m_b(M_Z)$ and the sum in quadrature is listed in Table 3. Hadronisation uncertainties [14] were evaluated in a

Algorithm	$m_b(M_z)$	stat.	exp. syst.	had.	theor.
E	2.271	+ 0.488	+ 0.734	+ 0.217	+ 0.194
	0.629		0.952	1.483	0.189
E0	2.642	+ 0.493	+ 0.789	+ 0.187	+ 0.213
	0.562		1.082	1.637	0.226
P	4.056	+ 0.426	+ 0.619	+ 0.048	+ 0.047
	0.500		0.974	0.717	0.021
P0	3.720	+ 0.305	+ 0.510	+ 0.130	+ 0.056
	0.354		0.724	0.885	0.043
D	2.509	+ 1.028	+ 1.879	+ 0.287	+ 0.170
	1.255		2.001	0.049	0.195
G	2.415	+ 2.075	+ 2.761	+ 0.691	+ 0.195
	2.415		2.415	2.415	0.078

Table 3: Values of the running b-quark mass extracted from the SLD measurement of r^b for each of the six jet algorithms.

similar fashion and are listed in Table 3.

Additional theoretical uncertainties were investigated by varying the value of $s(M_z)$ within the range $0.115 \leq s(M_z) \leq 0.121$. The corresponding changes in $m_b(M_z)$ were at the level of $(10 \text{--} 20) \text{ MeV}/c^2$. The renormalisation scale was also varied within the range $M_z = 2 \text{ to } 2M_z$. The corresponding changes in $m_b(M_z)$ were at the level of $200 \text{ MeV}/c^2$ or less. For each algorithm these uncertainties were added in quadrature to define a theoretical uncertainty, which is listed in Table 3.

The six measured b-quark masses range from 2.3 to 4.1 GeV/c^2 , with an rms. deviation of $0.7 \text{ GeV}/c^2$; this scatter is larger than one might expect from these data given the strong correlations between measurements using different jet algorithms, suggesting some additional source of uncertainty. In order to quantify this issue we

Algorithm	E	E0	P	P0	D	G
E	1.00	0.70	0.67	0.65	0.61	0.49
E0		1.00	0.84	0.82	0.61	0.49
P			1.00	0.71	0.65	0.56
P0				1.00	0.52	0.41
D					1.00	0.64
G						1.00

Table 4: Statistical correlation coefficients between r^b measurements for each pair of jet- finding algorithms.

evaluated the statistical correlations among the r^b values determined using different jet algorithms. We repeated the analysis on subsets of both the data and the simulated data and calculated the correlation coefficients empirically. The data and simulation gave consistent results, and the average correlation coefficients are listed in Table 4. Each has a statistical uncertainty of ~ 0.03 . The four JADE-like algorithms show strong correlations with each other, in the range $0.65\{0.84$, as might be expected. Correlations between other pairs of algorithms are weaker, in the range $0.41\{0.65$.

We evaluated

$$\chi^2 = \sum_{ij} (r_i^b - f_i(m_b, M_z)) (V^{-1})_{ij} (r_j^b - f_j(m_b)); \quad (12)$$

where r_i^b (f_i) are the measured (calculated) double ratios, $i, j = E, E0, P, P0, D, G$, the error matrix is defined by $V_{ij} = c_{ij} \sigma_{ij}$, c_{ij} is the correlation coefficient given in Table 4, and σ_{ij} is the statistical error on r_i^b . For values of m_b, M_z around $2.9 \text{ GeV}/c^2$, which is the average of the results shown in Table 3, we obtained $\chi^2 = 42/6$, which indicates an inconsistency among the results from the different algorithms. We minimized χ^2 with respect to variation of m_b, M_z and obtained $\chi^2 = 22/5$ for $m_b, M_z = 1.1 \text{ GeV}/c^2$, which is still unacceptably high. The best-fit χ^2 value is

insensitive to variations of the c_{ij} within their uncertainties, and to (simultaneous) systematic shifts of the measured r_i within the experimental systematic errors and hadronisation and theoretical uncertainties. The experimental systematic errors are dominated by uncertainties in the flavor composition of the samples, which we assume to be 100% correlated among all algorithms. We took the hadronisation uncertainties to be 100% correlated and the theoretical uncertainties to be completely uncorrelated.

We repeated this minimisation procedure and omitted in turn the measurement based on each of the six algorithms. In no case did we obtain a χ^2 value better than 12, which corresponds to a confidence level of roughly 1%. We then omitted pairs of measurements in turn. χ^2 values of less than 5, i.e. 10% confidence level, were obtained only for the six cases where any two of the E, E0, P and P0 algorithms were omitted; the corresponding mass values were in the range $2.46 \leq m_b(M_z) \leq 2.69 \text{ GeV}/c^2$. To the extent that the hadronisation and theoretical uncertainties have been properly estimated, we do not have a priori justification for omitting any particular algorithm (s). We do note, however, that algorithms in the JADE family have a significantly worse soft gluon behaviour than the D and G algorithms [23]. The former algorithms tend to combine soft gluons to form an 'artificial' jet at values of y_c that are not small, which may cause large higher-order perturbative corrections even for moderate values of y_c .

The χ^2 value is, however, quite sensitive to small changes in the measured r_i^b or predicted f_i . As an exercise, we have postulated an additional uncertainty of size ϵ which is uncorrelated between different jet algorithms. Under the hypothesis $m_b = 2.94 \text{ GeV}/c^2$, which is the average of the values listed in Table 3, for $\epsilon = 0.015$ the χ^2 value is 10; for $\epsilon = 0.02$ the χ^2 value is 7, which is acceptable. For $\epsilon = 0.02$ a fit for $m_b(M_z)$ yields a stable value of roughly $2.6 \text{ GeV}/c^2$, indicating that a consistent $m_b(M_z)$ value can be obtained provided that there exist additional uncertainties, uncorrelated between jet algorithms, at the level of 2% on r^b . A 2% error on the predicted r^b corresponds to an error of $0.5 \text{ GeV}/c^2$ on the extracted value of $m_b(M_z)$ from a given algorithm, and would roughly account for the $0.7 \text{ GeV}/c^2$ rms deviation among the values in

Table 3.

We suspect that the most likely source of the inconsistency among results for the different jet algorithms is the missing higher-order perturbative contributions to r^b . As we have shown, these would have to be only at the level of 2% in order to resolve the inconsistency. Possible NNLO contributions to r^b of this small magnitude are not a priori unexpected; 5{10% level NNLO contributions are implied by the scatter among $s(M_z)$ values determined using these and closely-related event-shape observables [18] which form the numerator and denominator of r^b .

4. Summary and Conclusions

We have studied the determination of the running b-quark mass by comparing NLO perturbative QCD calculations of the 3-jet ratio $\hat{r} = R_3^b = R_3^{\text{uds}}$ with data from the SLD Collaboration. We used six different infra-red- and collinear-safe jet-finding algorithms in order to study systematic effects. We find algorithm-dependent values of $m_b(M_z)$ in the range $2.3 < m_b(M_z) < 4.1 \text{ GeV}/c^2$. The value determined using the Durham algorithm is consistent with that reported in [13].

We quantified the statistical, experimental systematic, hadronisation and additional theoretical uncertainties, and attempted to obtain a best-fit $m_b(M_z)$ value by minimising χ^2 , taking statistical correlations between the results from the different algorithms into account. We could not obtain an acceptable best-fit χ^2 value unless we omitted any pair of the E, E0, P and P0 algorithms. In the absence of an a priori reason to do this we retained all six algorithms in order to investigate possible additional systematic effects. We were able to obtain an acceptable value of χ^2 , and a stable value $m_b(M_z) = 2.6 \text{ GeV}/c^2$, provided that we postulated (an) additional source(s) of uncertainty of relative size 2% on \hat{r} , which is uncorrelated between algorithms. We are unable to account for the origin of such an uncertainty, but speculate that it may be due to

uncalculated higher-order pQCD contributions.

We now discuss the assignment of a single value of $m_b(M_Z)$. Taking an unweighted average of the m_b values in Table 3, yields $m_b(M_Z) = 2.94^{+0.80}_{-0.95}$ (stat.) $^{+1.21}_{-1.36}$ (syst.) $^{+0.26}_{-1.20}$ (had.) $^{+0.14}_{-0.12}$ (theor.) 0.70 (rm s.) GeV/c^2 , where we include the rm s. deviation as an additional error. Though well defined, this procedure does not make full use of the information contained in the six measurements. The χ^2 minimisation procedure does take into account the full statistical covariance matrix, as well as correlations in the systematic error and hadronisation uncertainties. Since the resulting χ^2 is acceptable, and the fitted $m_b(M_Z)$ value is stable for any additional uncorrelated uncertainties of size ± 0.02 , we choose $\chi^2 = 0.02$, and obtain $\chi^2 = 7.0/5$ with

$$m_b(M_Z) = 2.52 \quad 0.27 \text{ (stat.)}^{+0.33}_{-0.47} \text{ (syst.)}^{+0.54}_{-1.46} \text{ (theor.)} \text{ GeV} = c^2 : \quad (13)$$

We consider that this represents our best estimate of the running b-quark mass using the SLD data.

The statistical error on $m_b(M_Z)$ is substantially reduced by the correlations among the six individual r^b results. The experimental systematic error is also reduced by the fact that a given shift of r^b causes the $m_b(M_Z)$ values for the E, E0, P and P0 algorithms to shift in opposite directions to those for the D and G algorithms. The theoretical uncertainty comprises the sum in quadrature of the hadronisation uncertainty ($^{+0.28}_{-1.39} \text{ GeV}/c^2$), and the propagation of the uncorrelated error of ± 0.02 on each r^b ($\pm 0.46 \text{ GeV}/c^2$). Variations of s and c contribute an uncertainty of $^{+0.14}_{-0.12} \text{ GeV}/c^2$; under the assumption that the 'error' results from uncalculated higher-order pQCD contributions the effects represented by these variations are already 'counted', and we have not added them in quadrature with the other theoretical uncertainties. Their inclusion does not change the central $m_b(M_Z)$ value and increases the total theoretical uncertainty to $^{+0.56}_{-1.47} \text{ GeV}/c^2$.

Our result is in agreement with that from [13]. The latter measurement has a significantly smaller theoretical uncertainty. For the Durham algorithm alone we would obtain an uncertainty of similar size, but our study of six different jet algorithms has

revealed additional systematic effects which warrant further investigation.

Acknowledgements

P.N.B., D.M. and N.O. thank colleagues in the SLD Collaboration for their support for this work. We thank Werner Bernreuther, Otfmar Biebel, and Mike Seymour for helpful discussions.

References

- [1] H. Fritzsch, M. Gell-Mann and H. Leutwyler, *Phys. Lett.* **47B** (1973) 365;
D.J. Gross and F.W. ilczek, *Phys. Rev. Lett.* **30** (1973) 1343;
H.D. Politzer, *Phys. Rev. Lett.* **30** (1973) 1346;
S. Weinberg, *Phys. Rev. Lett.* **31** (1973) 494.
- [2] R.K. Ellis, D.A. Ross, and A.E. Terrano, *Nucl. Phys. B* **178** (1981) 421;
K. Fabricius, I. Schmitt, G. Kramer, and G. Schierholz, *Z. Phys. C* **11** (1981) 315;
J.A.M. Vermaasen, K.J.F. Gaemers, and S.J.O. Ildham, *Nucl. Phys. B* **187** (1981) 301;
Z. Kunszt, *Phys. Lett. B* **99** (1981) 429;
G. Kramer and B. Lampe, *Fortschr. d. Phys.* **37** (1989) 161.
- [3] Z. Kunszt and P. Nason, "QCD" in *Z Physics at LEP 1*, eds. G. Altarelli, R. Kleiss, and C. Verzagnassi, CERN Yellow Report 89-08 (1989), Vol. 1, p. 373.
- [4] W.T. Giele, E.W.N. Glover, *Phys. Rev. D* **46** (1992) 1980.
- [5] S. Catani, M.H. Seymour, *Phys. Lett. B* **378** (1996) 287.

[6] S. Catani, M. H. Seymour, *Nucl. Phys. B* 485 (1997) 291.

[7] S. Frixione, Z. Kunszt, and A. Signer, *Nucl. Phys. B* 467 (1996) 399.

[8] Z. Nagy and Z. Trocsanyi, *Nucl. Phys. B* 486 (1997) 189.

[9] W. Bremmether, A. Brandenburg, P. Uwer, *Phys. Rev. Lett.* 79 (1997) 189;
A. Brandenburg, P. Uwer, *Nucl. Phys. B* 515 (1998) 279.

[10] G. Rodrigo, A. Santamaría, M. Bilenky, *Phys. Rev. Lett.* 79 (1997) 193; *hep-ph/9905276*.

[11] P. Nason, C. Oleari, *Phys. Lett. B* 407 (1997) 57; *Nucl. Phys. B* 521 (1998) 237.

[12] P. N. Burrows, SLAC-PUB-7914 (1998); to appear in *Proc. XXIX International Conf. on High Energy Physics, Vancouver, Canada, July 23-29 1998*.

[13] DELPHIC Collab., P. Abreu et al., *Phys. Lett. B* 418 (1998) 430.

[14] SLD Collab., K. Abe et al., *Phys. Rev. D* 59 (1999) 012002.

[15] OPAL Collab., contributed paper 295 to XXIX International Conf. on High Energy Physics, Vancouver, Canada, July 23-29 1998.

[16] W. A. Bardeen, A. J. Buras, D. W. Duke, T. Muta, *Phys. Rev.* 18 (1978) 3998;
D. W. Duke, *Rev. Mod. Phys.* 52 (1980) 199.

[17] N. Brown, W. Stirling, *Z. Phys. C* 53 (1992) 629.

[18] See eg. P. N. Burrows, *Proc. XXVIII International Conference on High Energy Physics, Warsaw, Poland, July 25-31 1996*, Eds. Z. Adjuk, A. K. Wroblewski, *World Scientific* 1997, p. 797.

[19] SLD Collaboration: K. Abe et al., *Phys. Rev. D* 51 (1995) 962.

[20] A LEPH Collab., D. Decamp et al., *Phys. Lett. B* 284 (1992) 163;
 L3 Collab., O. Adriani et al., *Phys. Lett. B* 284 (1992) 471;
 OPAL Collab., P D. Acton et al., *Z. Phys. C* 55 (1992) 1;
 DELPHIC Collab., P. Abreu et al., *Z. Phys. C* 59 (1993) 21.

[21] T. Sjöstrand, *Comp. Phys. Commun.* 82 (1994) 74;
 G. Marchesini et al., *Comp. Phys. Comm.* 67 (1992) 465.

[22] P N. Burrows et al., *Phys. Lett. B* 382 (1996) 157.

[23] S. Bethke et al., *Nucl. Phys. B* 370 (1992) 310; erratum : *ibid. B* 523 (1998) 681.

[24] JADE Collab., W. Bartel et al., *Z. Phys. C* 33 (1986) 23.

[25] B. L. Ioie, *Phys. Lett. B* 78 (1978) 277.

[26] W. T. Giele, E. W. N. Glover, D. A. Kosower, *Nucl. Phys. B* 403 (1993) 633.

[27] We thank M. Spira for a discussion of this point.

[28] A. Ballestrero, E. Maina, S. Moretti, *Phys. Lett. B* 294 (1992) 425.

[29] A. Signer, L. Dixon, *Phys. Rev. Lett.* 78 (1997) 811;
 L. Dixon, A. Signer, *Phys. Rev. D* 56 (1997) 4031;
 J M. Campbell, E W. Glover, D J. M. Hiller, *Phys. Lett. B* 409 (1997) 503;
 Z. Bern, L. Dixon, D A. Kosower, S. Weinzierl, *Nucl. Phys. B* 489 (1997) 3;
 Z. Nagy, Z. Trocsanyi, *Phys. Rev. Lett.* 79 (1997) 3604 ;
 Z. Nagy, Z. Trocsanyi, *Phys. Rev. D* 59 (1999) 014020;
 Z. Nagy, Z. Trocsanyi, *Nucl. Phys. Proc. Suppl.* 64 (1998) 63;
 S. Weinzierl, D A. Kosower, NIKHEF-99-002, SPHT-T 99/004, *hep-ph/9901277*.

[30] K. Hagiwara, T. Kurumada, Y. Yamada, *Nucl. Phys. B* 358 (1991) 80.

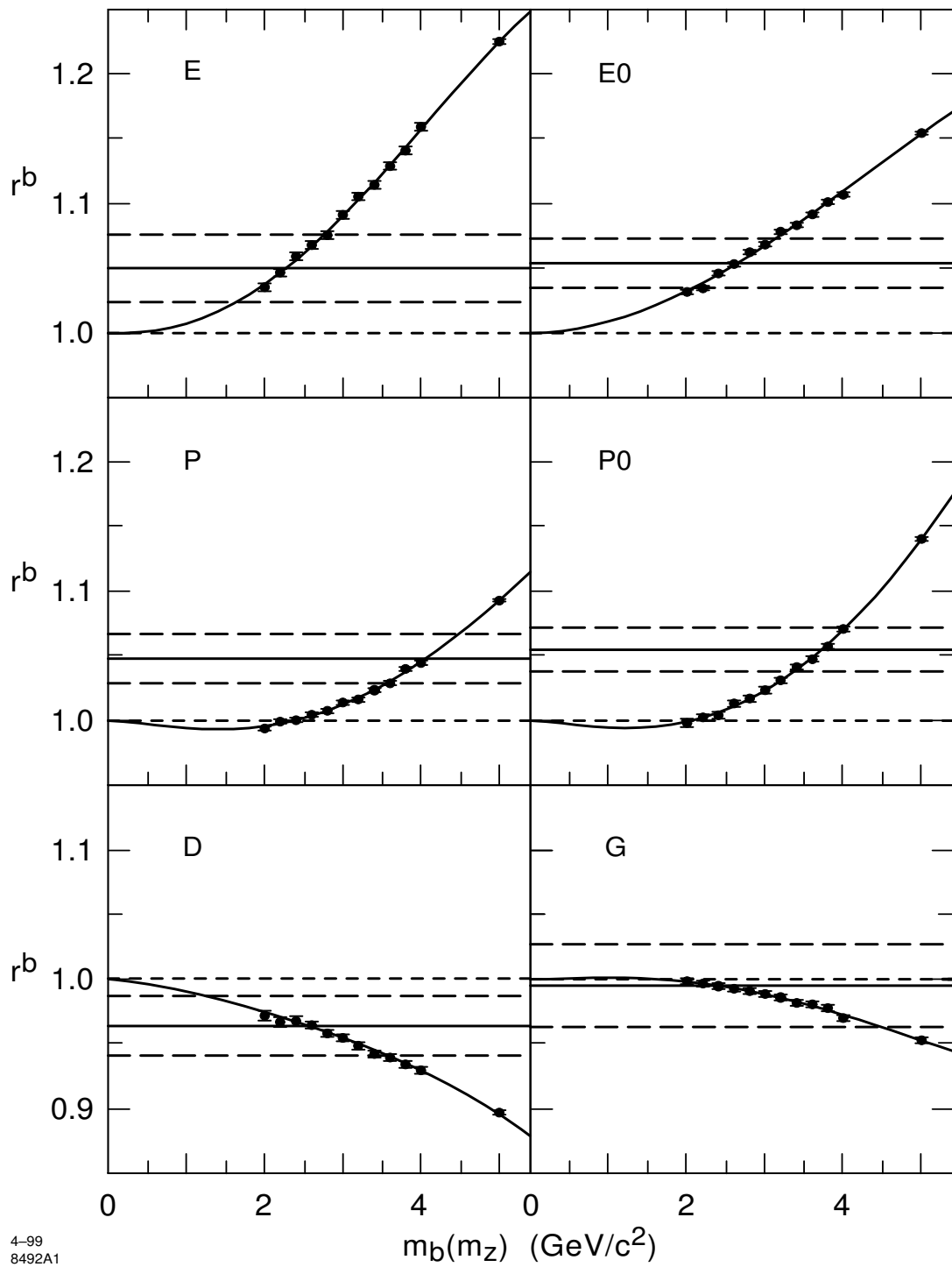


Figure 1: The $R_3^b = R_3^{uds}$ ratios measured by SLD for each of the six jet finding algorithms (horizontal bands) compared with the predicted dependence on the running b-quark mass, $m_b(M_Z)$.